Wakefields/Impedances for a Bunch Moving Between Two Corrugated Plates

Karl Bane

SLAC National Accelerator Laboratory

ICFA mini-Workshop on Impedances and Beam Instabilities in Particle Accelerators

18–22 September 2017

Benevento, Italy

Introduction

• The RadiaBeam/SLAC dechirper has been installed and commissioned at the Linac Coherent Light Source (LCLS). It consists of two pairs of flat, corrugated plates with the beam passing between them.

The flat geometry allows for adjustment of the strength of the dechirper. Having both a horizontal and vertical module allows for cancellation of unavoidable quad wake effects

• At the LCLS, which doesn't generally need more chirp control, the dechirper has, instead, been used more as a fast kicker, to facilitate a two-color mode of running the machine

• Analytical formulas for the longitudinal and transverse wakes have been developed to make it easier to do parameter studies and to plan the effective use of the dechirper

• These recent results are better than the perturbation calculations of the past. Note: we are here interested in very high frequency impedances since $\sigma_z \sim 10\ \mu$m, or $f \sim c/(2\pi\sigma_z) = 5.$ THz

Outline

- Corrugated structure as a dechirper
- Surface impedance calculation
- Wake measurements of RadiaBeam/SLAC dechirper at the LCLS
- Conclusions

• Much of the theory done with G. Stupakov, I. Zagorodnov, E. Gjonaj; see *e.g.* K. Bane, G. Stupakov, and I. Zagorodnov PRAB 19, 084401 (2016), and K. Bane, G. Stupakov, and E. Gjonaj, PRAB 20, 054403 (2017)

• Many people at SLAC were involved in the measurements. See also J. Zemella et al, SLAC-PUB-17121, August 2017, submitted to PRAB

X-RAY LIGHT SOURCES

XFEL System

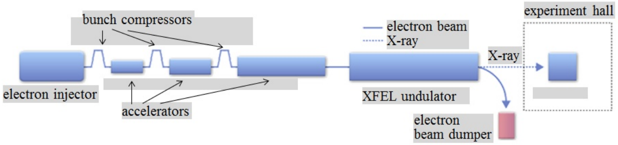

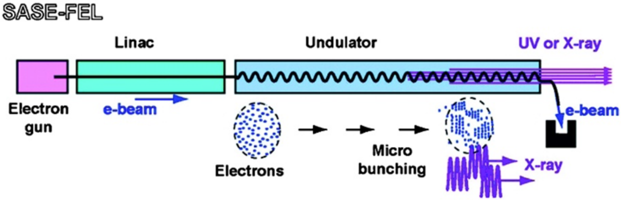

http://xfel.riken.jp/eng/sacla/index00.html
T.Shintake, Journal of JSSRR, Vol.18, No.1 (2005), p.35

LCLS-I Schematic

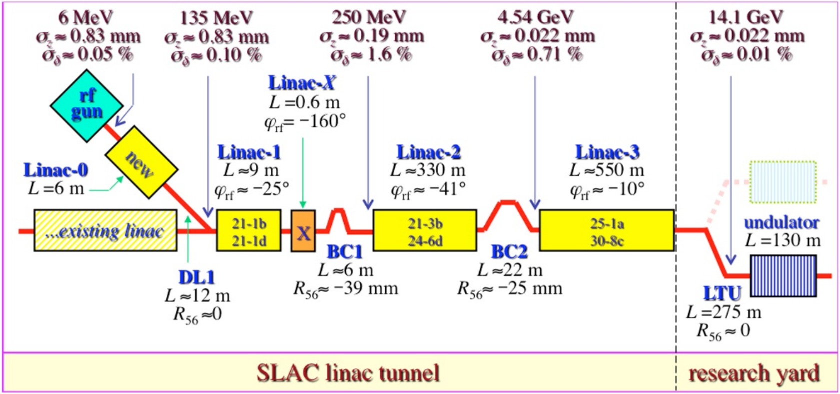

(P. Emma)

What is a Dechirper?

- In a linac-based, X-ray FEL, by the use of accelerating structures and chicanes, a low energy, low (peak) current beam (~ 10 MeV, ~ 100 A) is converted to one with high energy and high current (~ 5–10 GeV, ~ 1 kA). After the last bunch compressor the beam is typically left with an energy–longitudinal position correlation (an energy "chirp"), with the bunch tail at higher energy than the head

- A typical value might be $\nu = 40$ MeV/mm. To cancel this chirp, one can run off-crest in downstream RF cavities. Running the beam on the zero crossing of the wave, we would need length $L = \nu/(G_{rf}k_{rf})$ of extra RF. Or with peak RF gradient $G_{rf} = 20$ MeV/m, wave number $k_{rf} = 27$/m (for frequency $f = 1.3$ GHz), we would need $L = 74$ m of extra active RF

- Can we use the wakefields induced in a few meters of structure (in a "dechirper") to passively accomplish the same result?

Wakefield

Let us consider periodic structures with boundaries made of metal or dielectrics; *e.g.* resistive pipes, dielectric tubes, periodic cavities

• A driving charge Q passes at speed c through a structure. A test charge moves on a parallel trajectory also at speed c, at distance s behind. The longitudinal (point charge) wakefield $w(s)$ is the energy loss of the test particle per unit charge per unit length of structure

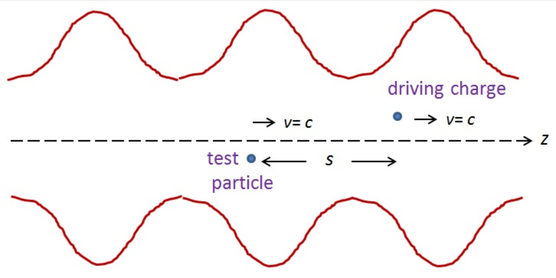

A driving and test particle move at $v = c$ in a periodic structure.

Wake at Origin

- The point charge wake, for structure period p, is

$$w(s) = -\frac{1}{Qp}\int_0^p E_z(z,t)\Big|_{t=(s+z)/c} dz$$

- For a periodic structure, the wake approaches a finite constant as $s \to 0$: $w_0 \equiv w(0^+)$. The constant w_0 depends only on the shape and size of the aperture (*e.g.* iris radius in periodic cavity) and on the (transverse) location of the particles.

For example, in a round structure, with the particles moving on axis, $w_0 = Z_0 c/(\pi a^2)$, with $Z_0 = 377\ \Omega$ and a the radius of the aperture. On axis in flat geometry, $w_0 = (\frac{\pi^2}{16}) Z_0 c/(\pi a^2)$

Ideal Dechirper

- For an X-ray FEL, an ideal dechirper would have the wake: $w(s) = w_0 H(s)$, with $H(s) = 0$ (1) for $s < 0$ ($s > 0$).

Why? At the end of an X-ray FEL the bunch distribution is (approximately) uniform: $\lambda(s) = H(s + \ell/2)H(\ell/2 - s)/\ell$, with ℓ the full bunch length.

Bunch wake

$$W_\lambda(s) = -\int_0^\infty w(s')\lambda(s - s')\, ds'$$

For ideal dechirper and uniform bunch distribution, $W_\lambda(s) = -w_0 s/\ell$, which is linear in s with tail losing most energy. Induced chirp, $\nu = -QLw_0/\ell$, with Q charge, L length of structure

- Resistive beam pipe or periodic cavities do not work well as dechirper, since the wake $w(s)$ drops quickly as s moves away from the origin

Corrugated Structure as Dechirper

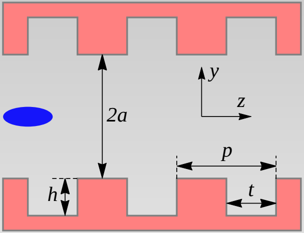

Geometry of a dechirper showing three corrugations. The blue ellipse represents an electron beam propagating along the z axis. For the RadiaBeam/LCLS dechirper, (typical) half-gap $a = 0.7$ mm, $h = 0.5$ mm, $p = 0.5$ mm, and $t = 0.25$ mm

• Perturbation calculation: round metallic pipe with small corrugations ($h, p \ll a$ and $h \gtrsim p$) has single mode wake: $w(s) \approx H(s) w_0 \cos ks$, with $k = 1/\sqrt{ah}$. With proper choice of parameters, can function as a good dechirper for an X-ray FEL

Round Numerical Example–NGLS

- We performed a time-domain wake calculation using I. Zagorodnov's ECHO code. Here $a = 3$ mm, $h = 0.45$ mm, $p = 1$ mm, $Q = 300$ pC, $\ell = 150$ μm, $L = 8.2$ m

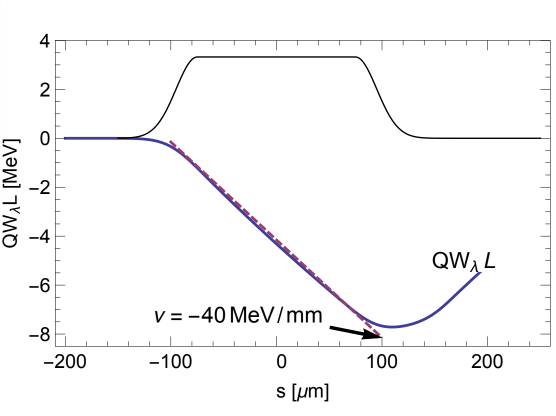

Dechirper for NGLS: wake of model of NGLS bunch distribution (blue). The dashed, red line gives the linear chirp approximation. The bunch shape λ, with the head to the left, is given in black

Impedances; Case of Flat Geometry

• Impedance, for wavenumber $k = \omega/c$ is given by the Fourier transform of the wake

$$Z(k) = \tilde{w}(k) = \frac{1}{c}\int_0^\infty w(s)e^{iks}\, ds$$

• Transverse wakes and impedances are given similarly to longitudinal ones. From Panofsky-Wenzel Theorem, the vertical dipole impedance is give by

$$Z_y = \frac{1}{k}\frac{\partial Z}{\partial y}$$

• Typically we are interested in wakes of *pencil beams*, *i.e.* of beams with small vertical extent. In flat geometry, with aperture at $y = \pm a$, transverse wakes and impedances are of form:

$$w_y(s) = y_0\, w_d(s) + y\, w_q(s)\ , \quad w_x(s) = w_q(s)(x_0 - x)\ ,$$

with driving charge at $(x_0, y_0) \ll a$, test charge at $(x, y) \ll a$

Surface Impedance Approach

• If corrugations are small ($h \ll a$), fields can be solved using surface impedance approach; *i.e.* on the walls we can let

$$\tilde{E}_z(k) = \zeta(k)\tilde{H}_\phi(k) \ ,$$

with $\zeta(k)$ the surface impedance

For corrugated structure, at high frequency, $\zeta(k) = -ihk/2$

• In flat geometry can obtain *generalized impedance* in form:

$$Z(x_0, y_0, x, y, k) = \int_0^\infty dq\, f(q, y, y_0, k, \zeta) e^{-iq(x-x_0)} \ ,$$

where driving and test particles can be anywhere in the aperture, and f is an explicit, analytical function

(However, normally we are interested in pencil beams, *i.e.* where $x \approx x_0$, $y \approx y_0$)

Surface Impedance Cont'd

- The same has been done for the transverse impedance. By then performing two numerical integrals, we obtain an estimate of the generalized longitudinal and transverse wakes

- By letting $a-y=b$ and letting $a\to\infty$ (a is half-aperture of two jaws) we obtain the wakes of a beam passing by a single dechirper jaw at distance b

- The only problem is, the surface impedance approach is valid when $(h/a)\ll 1$, but here nominally $(h/a)=(0.5/0.7)=0.7\not\ll 1$ (and similarly for the single jaw case)

However, these calculations, when applied to LCLS-type parameters, seem to agree well with numerical time-domain simulations (ECHO(2D) by I. Zagorodnov [double jaws] and CST Studio by E. Gjonaj [single jaw])

- We have further simplified the results by extracting (analytical) parameters and using *e.g.* $w(s)=w_0H(s)$ (*zeroth order*—less accurate) and $w(s)=w_0H(s)e^{-\sqrt{s/s_0}}$ (*first order*—more accurate)

Surface Impedance Cont'd

- Similar for transverse (dipole and quad) wakes are of form

$$w_y(s) = 2w'_{0y} H(s) s_{0y} \left[1 - \left(1 + \sqrt{\frac{s}{s_{0y}}}\right) e^{-\sqrt{s/s_{0y}}}\right]$$

- To obtain *e.g.* w_0 from $Z(k)$: note that high frequency, asymptotic form of impedance

$$Z_a(k) = \frac{w_0}{c} \int_0^\infty ds\, e^{iks} = \frac{iw_0}{kc}$$

So

$$w_0 = -ikcZ_a(k) = -ic \lim_{k\to\infty} kZ(k)$$

which is a positive constant

- Parameter s_0 can also be derived in analytical form from structure of impedance of periodic device at high frequencies

Two-Plate Example, with Half-Gap $a = 0.7$ mm

$$w_{yq}(s) \approx \frac{\pi^4}{16a^4} s_{0q} \left[1 - \left(1 + \sqrt{\frac{s}{s_{0q}}} \right) e^{-\sqrt{s/s_{0q}}} \right]$$

$$s_{0q} = \frac{a^2 t}{2\pi\alpha^2 p^2} \left(\frac{15}{16} \right)^2 , \quad \text{with} \quad \alpha \approx 1 - 0.465\sqrt{\zeta} - 0.070\zeta \Big|_{\zeta = t/p}$$

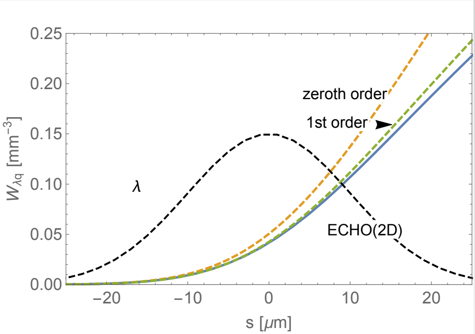

Quad bunch wake for a Gaussian beam on axis, with $\sigma_z = 10\ \mu$m, in the RadiaBeam/LCLS dechirper. Given are the numerical results of ECHO(2D) (blue), and the analytical zeroth order (red) and 1st order results (green). The bunch shape $\lambda(s)$ is shown in black

Single Plate Example

$$w_{yd}(s) = \frac{2}{b^3} s_{0y} \left[1 - \left(1 + \sqrt{\frac{s}{s_{0y}}} \right) e^{-\sqrt{s/s_{0y}}} \right] ,$$

with $s_{0y} = 8b^2 t/(9\pi\alpha^2 p^2)$

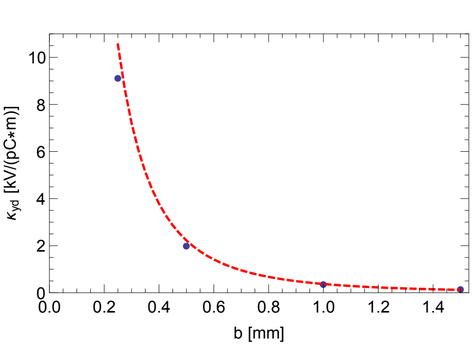

Single plate dipole kick factor $\varkappa_{yd}$ as function of distance of the beam from the wall b, showing the CST results (blue symbols) and those of the analytical model (red dashes). The bunch is Gaussian with length $\sigma_z = 100\ \mu m$

RadiaBeam/LCLS Dechirper Installed in LCLS

(From right to left) the beam passes through: the vertical dechirper module, a quad, and the horizontal module

RadiaBeam/LCLS Dechirper: Horizontal Module Detail

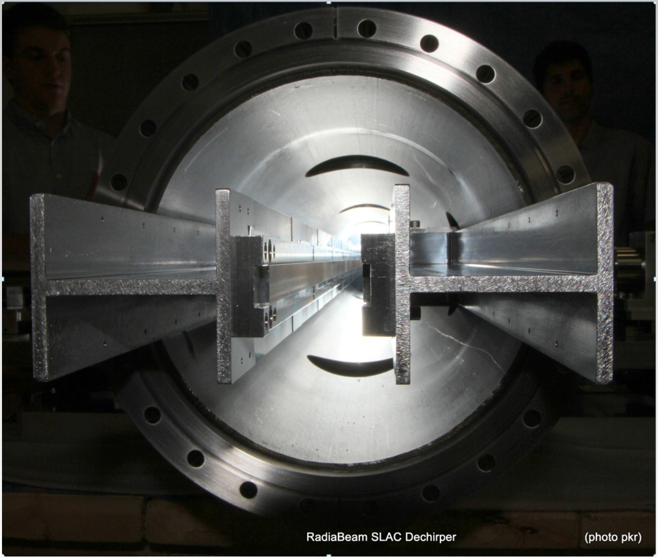

Detail showing the corrugated plates and their supports

RadiaBeam/LCLS Dechirper: Corrugation Details

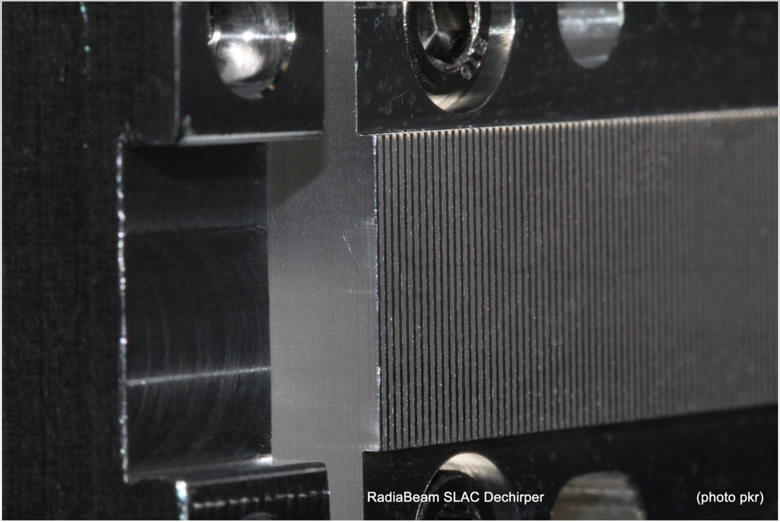

Detail of the beginning of a corrugated plate

Beam Line Layout for Dechirper Wake Measurements

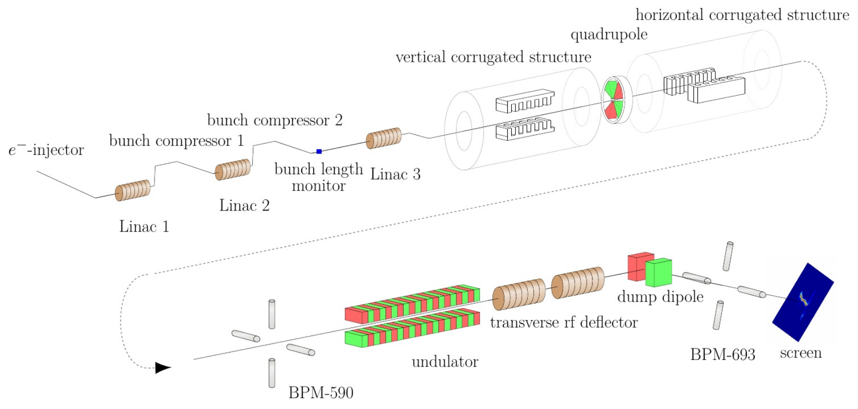

Sketch of LCLS beam line, focusing on the RadiaBeam/SLAC dechirper and the diagnostics used in the wake measurements. Note that the relative scale of distances is greatly distorted; in reality the linacs are much longer than the other objects shown.

Two-Plate Chirp Measurement

Single X-band deflector measurement:
@ 4.4 GeV / 180 pC / 1 kA

Data from dump screen

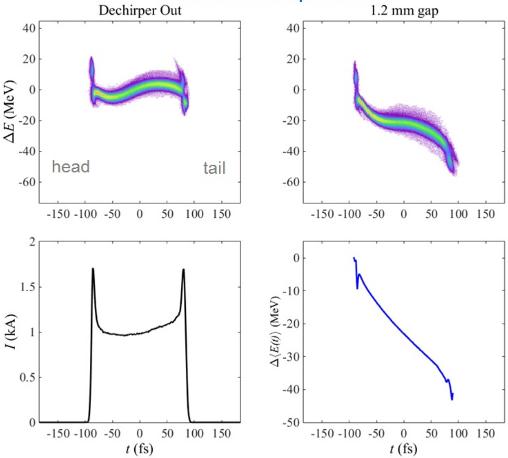

Obtained from data from dump screen

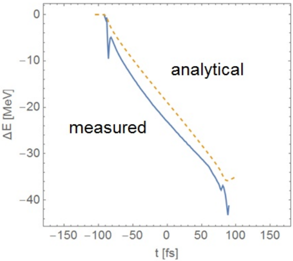

Clear, ~linear additional chirp observed

Using both dechirpers (L= 4 m)

(T. Maxwell)

Two Plates: Average Energy Loss Measurement

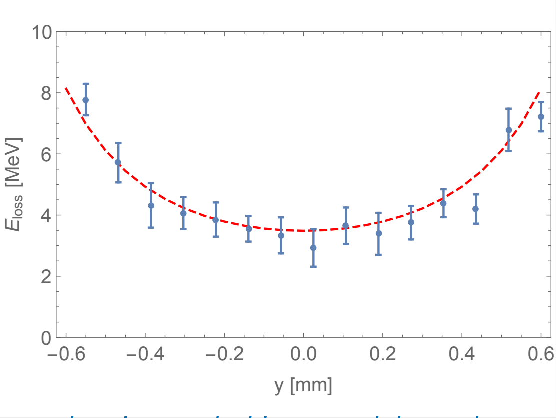

Average energy loss in one dechirper module vs. *beam transverse offset, showing measurement (symbols) and analytical theory (curve). Here half-gap $a = 1.1$ mm, structure length $L = 2$ m. For analytic curves, gap was reduced by 5% to fit to the data.*

- Bunch charge $Q = 190$ pC, peak current $I = 1$ kA, energy $E = 4.4$ GeV

Two Plates: Average Dipole Kick Measurement (1)

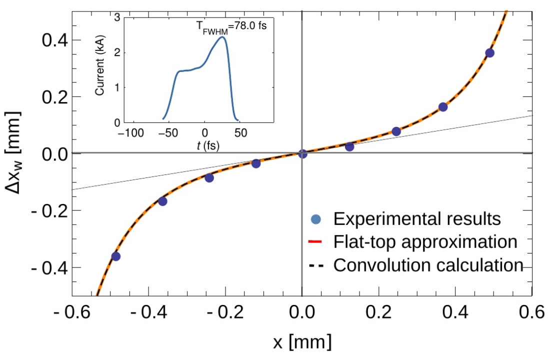

Downstream deflection, Δx_w, as function of offset in the (horizontal) dechirper, x, for half-gap $a = 1$ mm. For the analytic curves, the gap parameter was reduced by 11% to fit the experimental data. The bunch current, with head to the left, is shown in the inset.

- Bunch charge $Q = 152$ pC, energy $E = 6.6$ GeV

Two Plates: Average Dipole Kick Measurement (2)

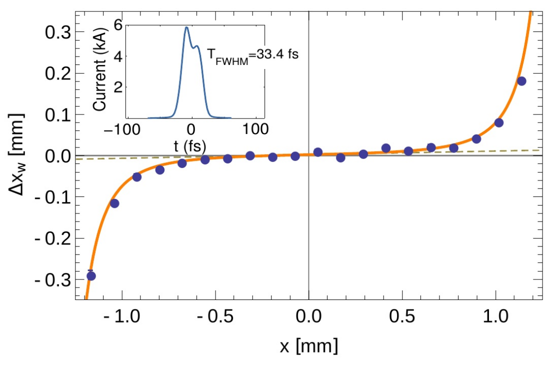

Downstream deflection, Δx_w, as function of offset in the dechirper, x, for half-gap $a = 1.55$ mm. For the analytic curve (flat-top approximation), the gap parameter was reduced by 6% to fit the experimental data. The bunch current, with head to the left, is shown in the inset.

- Bunch charge $Q = 187$ pC, energy $E = 13.3$ GeV

Single Plate: Average Kick Measurements

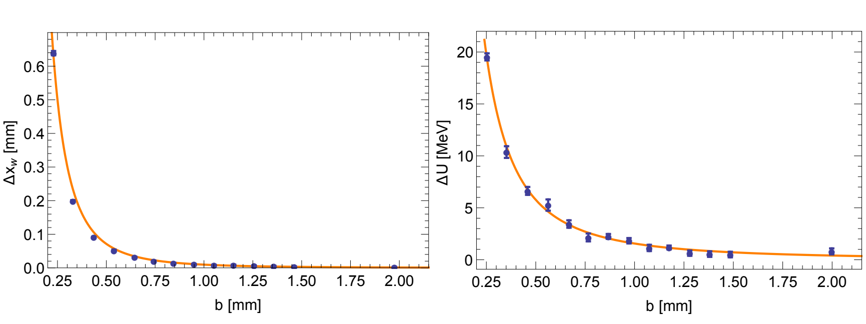

Downstream deflection, Δx_w (left), and energy loss, ΔU (right), as functions of beam offset from a single dechirper plate, b. The symbols give the data points, with their b values shifted by -161 μm (left), and -138 μm (right); the curves give the analytical theory. Here $Q = 180$ pC, $I = 3.5$ kA, $E = 13$ GeV.

- The absolute value of the measured offset, b, has some uncertainty. The fact that the two fitted shifts agree quite well is a confirmation of the theory and of the fitted shifts

Fresh-Slice, Two-color Idea

- A strong, differential dipole kick (no kick at the head, maximum kick at the tail) can be induced in the dechirper. This is done by passing the beam either off axis between two dechirper plates, or near to just a single plate
- This method was quickly made operational at the LCLS

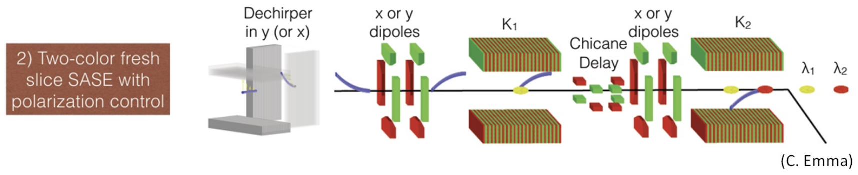

Sketch of Fresh-Slice, two-color operation at the LCLS using the dechirper. By steering the head or tail of the beam to the axis, the dipoles select which part lases in the immediately succeeding undulator. The chicane delay allows for adjustment of the time interval between the two (differently colored) pulses

Fresh-Slice Two-color Operation at the LCLS

Fresh-slice double-pulses:

Two color scheme, with color separation and tail lasing first

(A. Lutman)

SLAC

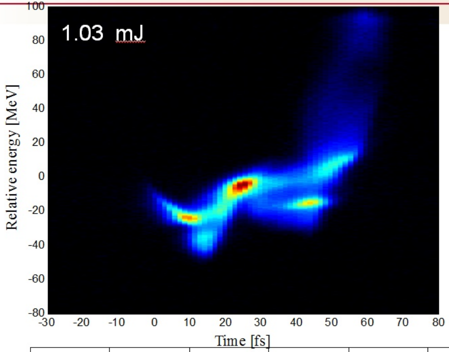

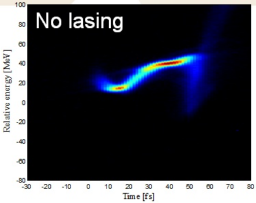

FEL Statistics:
746 +/- 125 μJ

Regular Taper
Delta in circular polarization

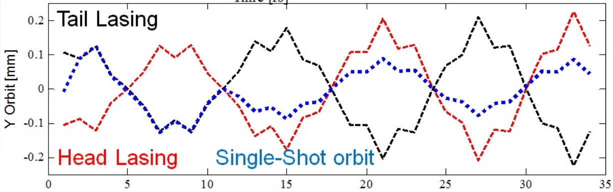

first color: ~250 μJ
second color: ~ 500 μJ

first color: ~8 fs
second color: ~ 15 fs

Conclusions

- The corrugated, metallic structure can be used for passive chirp control at the end of a linac-based, X-ray FEL

- It can also be used as a fast kicker, to facilitate two-color, Fresh-Slice operation of an FEL such as LCLS. (It is regularly being used for this purpose at the LCLS)

- Using the surface impedance approach we are able to obtain analytical solutions for the wakes of the structure: longitudinal, dipole, quad wakes; two-plate case, on axis and off; and single plate case

- These wakes agree well with numerical simulations for LCLS-type beam parameters, in spite of the fact the corrugation perturbation is not extremely small. They also agree quite well with measurements using the RadiaBeam/SLAC dechirper at the LCLS

Contributors to Installation and Commissioning of the RadiaBeam/LCLS Dechirper

FEL Physics	Radiabeam Systems	METS	Controls
T. Maxwell	M. Ruelas	A. Cedillos	A. Babbitt
P. Krejcik	M. Harrison	M.A. Carrasco	Z. Oven
M. Guetg	J. McNevin	G. Gassner	M. Petree
J. Zemella	D. Martin	E. Reese	J. Bong
Z. Huang	A. Murokh	K. Caban	M. D'Ewart
K. Bane	P. Frigola	S. Jansson	S. Hoobler
G. Stupakov		T. Montagne	S. Alverson
P. Emma		J. Garcia	L. Piccoli
J. Frisch		R. Atkinson	
H. Loos			
A. Lutman			
A. Fisher			
A. Novokhatski			
R. Iverson			